DOI: 10.1002/ejoc.200600916

Can Four-Membered Heterophosphete Structures Exist? The Contribution of Phosphorus d Orbitals to Antiaromaticity

Zoltán Mucsi,*[a] Tamás Kötvélyesi,[b] Béla Viskolcz,[c] Imre G. Csizmadia,[c,d]
Tibor Novák,[e] and György Keglevich[a]

Keywords: Heterophosphete / Ab initio calculations / Density functional calculations / Antiaromaticity / Aromaticity

The large instability of heterophosphete compounds, composed of a four-membered unsaturated ring with a pentavalent phosphorus atom and a heteroatom, has been identified and characterised by first-principle molecular orbital computations, at several levels of theory. It has been shown that strong electron-withdrawing groups bound to the phosphorus atom are able to stabilize the system. The extent of antiaromaticity of these compounds is examined and quantified by a linear aromatic and antiaromatic scale.

Introduction

Molecular structures are often influenced by aromatic stabilization and antiaromatic destabilization effects.[1] Antiaromaticity was formerly considered "homogenic" due to the involvement of similar p_z orbitals perpendicular to the planar ring. Cyclobutadiene[2] and its derivatives[1,3,4] are prime examples of antiaromatic compounds.[5] In this paper, we present selected phosphorus-containing compounds as examples where antiaromaticity is "heterogenic". Specifically, we present systems where not all of the participating orbitals are *p*-type orbitals, that is, d-type orbitals may also be included. The extent of antiaromaticity of the compounds examined is quantified by a linear, unified aromatic, as well as an established antiaromatic scale.[6] Heterophosphetes **1**, a group of four-membered β-heterocycles,[7,8] are structurally related to biologically active penicillin-type β-lactams. Heterophosphetes exist as two conformers (**1A** and **1B**) linked by pseudorotation (Scheme 1).[9,10] Their saturated counterparts, heterophosphetanes, may also exist as two conformers (**2A** and **2B**) and are well-known intermediates of the Wittig reaction.[11] The orientation of the substituents is controlled by the apofilicity properties of Y and X;[10] hence in the two **A** structures, Y–P is equatorial, whereas in the two **B** forms, Y–P is apical. Heterophosphetes **1A** and **1B** prefer to undergo ring-opening reactions to form structure **3**.[7,8] This may be one of the reasons that earlier synthetic attempts to produce heterophosphetes have often failed.[7,8] In contrast to **1A** and **1B**, compounds of types **2A** and **2B** never undergo ring-opening to form **4**. As a matter of fact, only two compounds (**5**[12] and **6**,[13] Figure 1) are representative of the heterophosphete family. According to X-ray crystallography, the N···P distance in **5** is 2.170 Å,[12] which is considerably longer than the sum of the covalent radii (1.06 Å + 0.75 Å = 1.81 Å). This stable compound can only be regarded to have structure **1B** in the loosest sense.

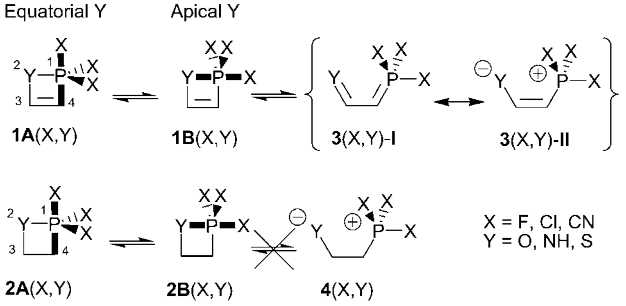

Scheme 1. Structure of heterophosphetes **1A** and **1B**. Heterophosphetanes **2A** and **2B** are also presented, as well as their ring-opened forms **3** and **4**, respectively.

---

[a] Department of Organic Chemical Technology, Budapest University of Technology and Economics,
1521 Budapest, Hungary
Fax: +36-1-4633648
E-mail: zoltanmucsi@gmail.com
[b] Department of Physical Chemistry, Faculty of Science, University of Szeged,
6725 Szeged, Hungary
[c] Department of Chemistry and Chemical Informatics, Faculty of Education, University of Szeged,
6725 Szeged, Hungary
[d] Department of Chemistry, University of Toronto,
Toronto, ON, Canada M5S 3H6, Canada
[e] Research Group of the Hungarian Academy of Sciences at the Department of Organic Chemical Technology,
1521 Bp. Hungary

Supporting information for this article is available on the WWW under http://www.eurjoc.org or from the author.

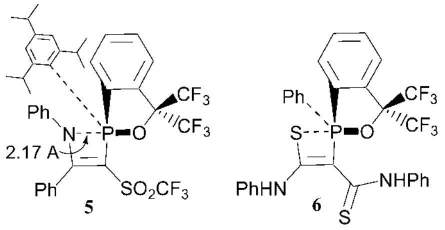

Figure 1. Prepared heterophosphetes **5** and **6**.

Computational Methods

The geometries and analytical frequencies were computed at the B3LYP level of theory by employing the 6-311++G(2d,2p)[14] basis set with the use of the Gaussian 03[15] program. For the determination of the 3D potential surfaces (PES), the B3LYP/6-31G(d) level of theory was used. The thermodynamic enthalpy values (H) were calculated at 298.14 K.

The exact description of the aromatic or antiaromatic character of the ring structures can be examined by different scales such as the HOMA index,[16] NICS values[17,18] and enthalpies of homodesmic reactions, which results in an aromatic stabilizing energy (ASE).[19] The determination of the antiaromatic character of heterophosphete **1** is not simple by traditional means. HOMA index requires reference bond lengths for completely aromatic and nonaromatic ring systems containing the same atoms in the ring. The NICS values show significant deviation from the usual values computed for carbocycles, which is due to the larger shielding effect of the large P atom combined with the small ring size. It should be noted that the NICS values are influenced by the exocyclic X substituents on the P^1 atom because of the steric proximity of the X-position as well as the point that is 1 Å above the ring centre. The results of homodesmic reactions may also be misleading as the configuration around the P atom changes during the ring opening reactions.

A further possibility is that aromaticity and antiaromaticity are characterised by a common and universal linear scale that is based on the enthalpy of hydrogenation [see ΔH_{H2} and $\Delta\Delta H_{H2}$ in Equations (1), (2) and (3)] when cyclobutadiene (**7**) and benzene (**10**) are considered as –100% and +100%, respectively.[6] This methodology compares the hydrogenation reaction of the examined compound with that of a properly chosen reference reaction.

$$\Delta H_{H2}(\text{examined}) = H[\mathbf{2}(X,Y)] - \{H[\mathbf{1}(X,Y)] + H(H_2)\} \quad (1)$$

$$\Delta H_{H2}(\text{reference}) = H[\mathbf{2}(X,CH_2)] - \{H[\mathbf{1}(X,CH_2)] + H(H_2)\} \quad (2)$$

$$\Delta\Delta H_{H2} = \Delta H_{H2}(\text{examined}) - \Delta H_{H2}(\text{reference}) \quad (3)$$

The hydrogenation methodology requires a reference hydrogenation reaction, where an unsaturated analogue that does not possess any aromatic or antiaromatic character is also hydrogenated [Equation (2)].

These equations are valid for both **A** and **B** conformers. It should be noted, however, that **2A**(X,CH$_2$) and **2B**(X,CH$_2$) are identical due to internal symmetry of the molecule. By considering these criteria, the hydrogenation of phosphetenes **1A**(X,CH$_2$) and **1B**(X,CH$_2$) that result in **2A**(X,CH$_2$) ≡ **2B**(X,CH$_2$) with the same X substituents were considered as the reference reaction of the hydrogenation of **1A** and **1B** (Figure 2, Table 2). Recall that compounds **2B** in most cases do not represent a minimum on

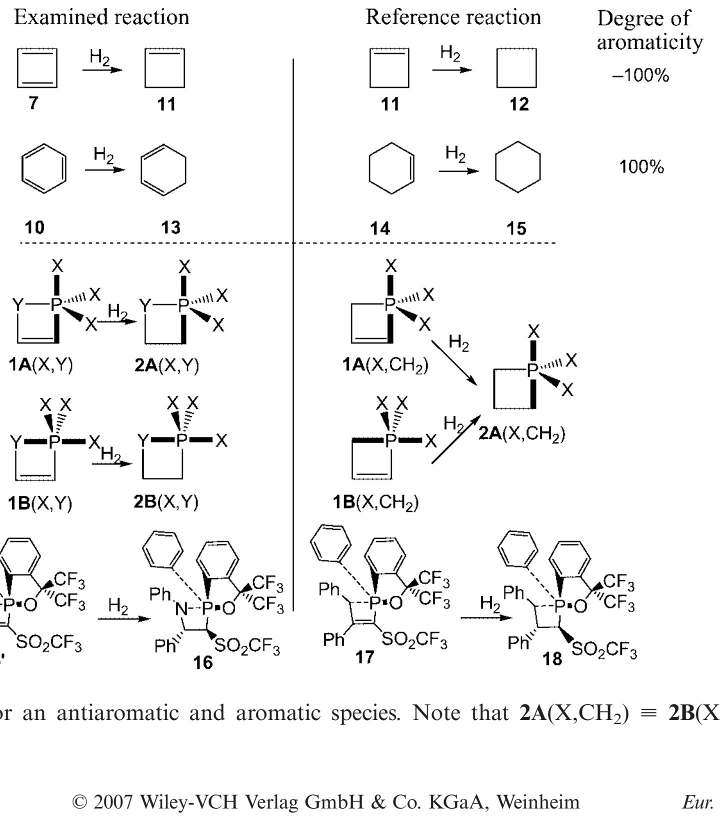

Figure 2. ΔH_{H2} vales calculated for an antiaromatic and aromatic species. Note that **2A**(X,CH$_2$) ≡ **2B**(X,CH$_2$) are identical due to internal symmetry.

the potential energy surface. In these cases, the optimised **2B*** structures with one imaginary frequency were used in the calculation of the ΔH_{H2} values for **1B[rarr]2B**.

Results and Discussion

The discussion is divided into several parts. The molecular and electronic stabilities of **1** and **2** will be discussed, followed by a consideration of the extent of their antiaromatic character.

Molecular Structure

The present study indicated that electron-withdrawing groups (EWG) as exocyclic substituents (X) can stabilize both **1A** and **1B** rings, whereas electron-donating groups (EDG) cannot. This is the first time when stable heterophosphetes are identified theoretically. This finding answers the question posed in the title of this paper; heterophosphetes can indeed exist provided that the molecular structure exhibits a favourable electron distribution. For this reason, we have examined conditions in which ligands X = F, Cl and CN were used. As far as Y is concerned, three cases were published in the literature where Y = NR, O or S. In this study, we considered the combination of the chosen three X substituents and these three Y heteroatomic moieties, which corresponds to 3 × 3 = 9 congeners. For the sake of comparison, both the unsaturated and saturated families were considered; therefore, 2 × 9 = 18 compounds were computed. For both families of compounds, there were two cyclic conformers (**A** and **B**), and together, there were 2 × 18 = 36 structures to study, regardless of their stability.

The $\Delta H_{\mathbf{A}\rightarrow\mathbf{B}}$ values for pseudorotation defined by Equations (4) and (5) for compounds **1** and **2**, respectively, and their relative values are specified in Equation (6). These data are presented in Table 1.

$$\Delta H_{\text{pseudo}}(\mathbf{1}) \equiv \Delta H_{\mathbf{1A}\rightarrow\mathbf{1B}} = H_{\mathbf{1B}} - H_{\mathbf{1A}} = H[\mathbf{1B}(\text{X,Y})] - H[\mathbf{1A}(\text{X,Y})] \quad (4)$$

$$\Delta H_{\text{pseudo}}(\mathbf{2}) \equiv \Delta H_{\mathbf{2A}\rightarrow\mathbf{2B}} = H_{\mathbf{2B}} - H_{\mathbf{2A}} = H[\mathbf{2B}(\text{X,Y})] - H[\mathbf{2A}(\text{X,Y})] \quad (5)$$

$$\Delta\Delta H_{\text{pseudo}} = \Delta H_{\text{pseudo}}(\mathbf{2}) - \Delta H_{\text{pseudo}}(\mathbf{1}) \quad (6)$$

The $\Delta H_{\mathbf{2A}\rightarrow\mathbf{2B}}$ values are usually positive or near zero [e.g. for **2**(F,O), $\Delta H_{\mathbf{2A}\rightarrow\mathbf{2B}}$ = 2.36 kJ mol^{-1}] as a consequence of the stronger conjugation of the equatorial Y^2 substituent. Thus, structures **2A** are, in general, more stable than **2B**, which is in agreement with the experimental findings. Computed $\Delta H_{\mathbf{1A}\rightarrow\mathbf{1B}}$ values for **1** are, however, negative and almost larger in their absolute values, which suggests that **1B** is the preferred isomer [e.g. for **1**(F,O), $\Delta H_{\mathbf{1A}\rightarrow\mathbf{1B}}$ = –40.53 kJ mol^{-1}].

The $\Delta H_{\mathbf{1A}\rightarrow\mathbf{1B}}$ values provide some measure of the stability of ring **1A** with respect to ring **1B** when compared to the $\Delta H_{\mathbf{2A}\rightarrow\mathbf{2B}}$ of ring **2A** with respect to ring **2B**. In this case, the CN group offers the greatest level of stabilization ($\Delta\Delta H_{\text{pseudo}}$) for all three heteroatoms (Y = NR, O and S). The best value appears to be **1A**(CN,NH), as shown in Figure 3.

Table 1. Computed ΔH values (kJ mol^{-1}) for the pseudorotation processes.

		ΔH_{pseudo}		$\Delta\Delta H_{\text{pseudo}}$[b]
Y	X	**1A→1B**	**2A→2B**	
O	F	–40.53	2.36	–42.89
	Cl	–47.71	–1.73	–45.98
	CN	–59.62	–6.24	–53.38
NH	F	–20.78	24.53[a]	–45.31
	Cl	–20.09	24.71[a]	–44.80
	CN	–38.98	17.66[a]	–56.64
S	F	–23.48	8.88[a]	–32.36
	Cl	–25.08	10.14[a]	–35.22
	CN	–46.50	–0.15[a]	–46.35

[a] Structure **2B** is a stationary point with one imaginary frequency. [b] $\Delta\Delta H_{\text{pseudo}}$ is defined by Equation (6).

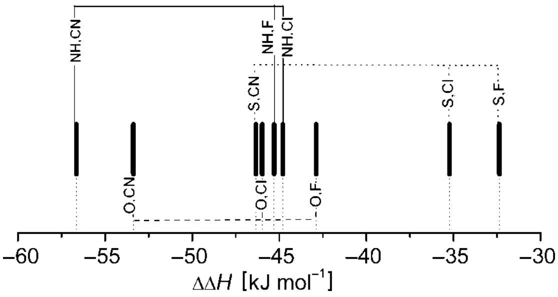

Figure 3. Computed $\Delta\Delta H_{\text{pseudo}}$ values for nine heterophosphete congeners.

The contrast in the stabilities of the species involved can be represented by the 3D PES for the **1A→1B→3** and **2A→2B→4** routes (Figure 4) when Y = O and X = F. In generating these PESs, two constraints were applied: one of which is the d = P^1–O^2 distance, whereas the second is the χ = X$_{\text{axial}}$–P^1–O^2–C^3 dihedral angle. Note that in the PES in Figure 4a, **1B** is more stable than **1A**, whereas in Figure 4b, **2A** is more stable than **2B**.

The question then arises as to why the stability of four-membered ring **1** decreases with the introduction of a double bond into the ring of **2**. It is not simply a consequence of the increased ring strain due to the presence of the double bond in the four-membered ring, which increases the ring strain by only about 20–25 kJ mol^{-1}.

All P^1–Y^2 distances are larger in both **1A** and **1B** by 0.05–0.1 Å than those in **2A** and **2B** (Table S1). In the case of azaphosphetanes **2** (Y = NH), however, the H atom attached to the N^2 atom is placed in the plane of the ring, and for azaphosphetes **1A** and **1B**, the symmetry of the molecule is broken and the NH group is bent out from the plane of the molecule.

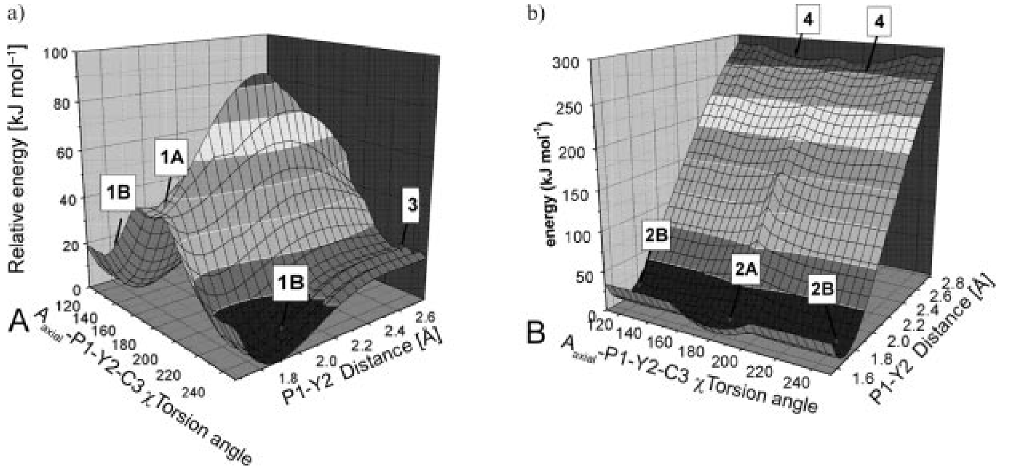

Figure 4. The 3D potential surfaces for the **1A**→**1B**→**3** and **2A**→**2B**→**4** transformations computed at the B3LYP/6-31G(d) level of theory.

Electronic Structure

Around the pentavalent phosphorus atom having trigonal-bipyramidal structure (sp^3d hybridisation state), the substituents may be equatorial or axial (Scheme 2). Traditionally, it is assumed that the lone pair of electrons of a heteroatom-containing moiety (e.g. an NH_2 group) in the equatorial position (**I**) may be delocalised into an unoccupied d atomic orbital (AO) of the adjacent phosphorus atom. If the NH_2 group is in the axial position (**II**), this conjugation is not significant; consequently, the two H atoms attached to the N atom, as well as the N and P atoms are not in the same plain as the N atom is in an sp^3 hybridisation state. The bond length between the P atom and an apical substituent is much longer [in **II**, d_{P-N} = 1.862 Å at the B3LYP/631G(d) level of theory] than the bond length between the P atom and an equatorial substituent (in **I** d_{P-N} = 1.717 Å). The situation is, however, analogous if d orbitals are not included in the basis set, as shown in Scheme 2.

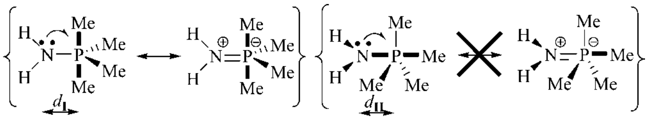

	I	II	$\Delta d_{II\text{-}I}$
B3LYP/6-31G(d)	1.717 Å	1.862 Å	0.145 Å
B3LYP/6-31G	1.787 Å	1.949 Å	0.162 Å

Scheme 2. Resonance structures and P–N atomic distances of **I** and **II** at different levels of theory.

The previously marked difference in stability between **1** and **2** can be explained by assuming the existence of an additional destabilizing electronic effect. In the case of **1A**, the conjugation between P^1 and equatorial Y^2 is larger and the ring involves 4π electrons. This results in increased antiaromaticity of the system that destabilizes **1A**. Hence, the system is relieved by pseudorotation to **1B**, where the apical Y^2–P^1conjugation is much less efficient. Accordingly, we found that compound **1** possesses strong antiaromatic characteristics, which have been observed in other nonisolable four-membered rings such as cyclobutadiene (**7**),[1–8] four-membered unsaturated lactones (**8**) and unsaturated lactams (**9**)[20] (Figure 5).

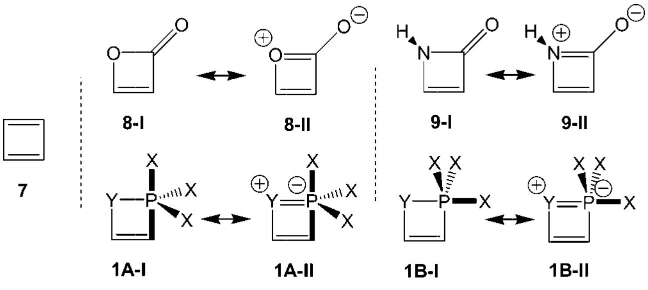

Figure 5. Resonance structures of some antiaromatic compounds.

This phenomenon has, however, not been examined in the group of phosphorus compounds up until now. This antiaromatic character originates from the significant conjugation of the p_z atomic orbital of Y^2 that contains an electron pair and that of an appropriately oriented empty d orbital of P^1 as previously suggested[20] for **8** and **9** (Figure 5). Consequently, the P^1–Y^2 bond order increases, which causes an unfavourable cyclobutadiene-like resonance structure for **1**, **8** and **9** (Figure 5).

In contrast to the usual stabilizing effect of this type of conjugation, which involves a pentavalent ring phosphorus, in this particular case, the system is destabilised as a result of the formation of a four-π-electron-containing, four membered, heterophosphete ring. Previously studied[1–8,20] antiaromatic structures (e.g. **7**, **8** and **9**) involve four overlap-

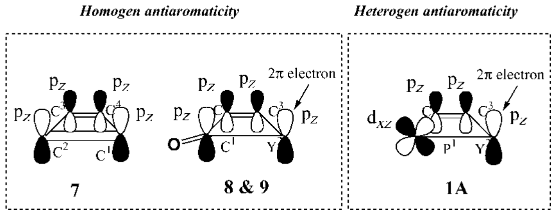

Figure 6. Atomic orbitals of **7**, **8**, **9**, and **1A**, which results in antiaromatic character.

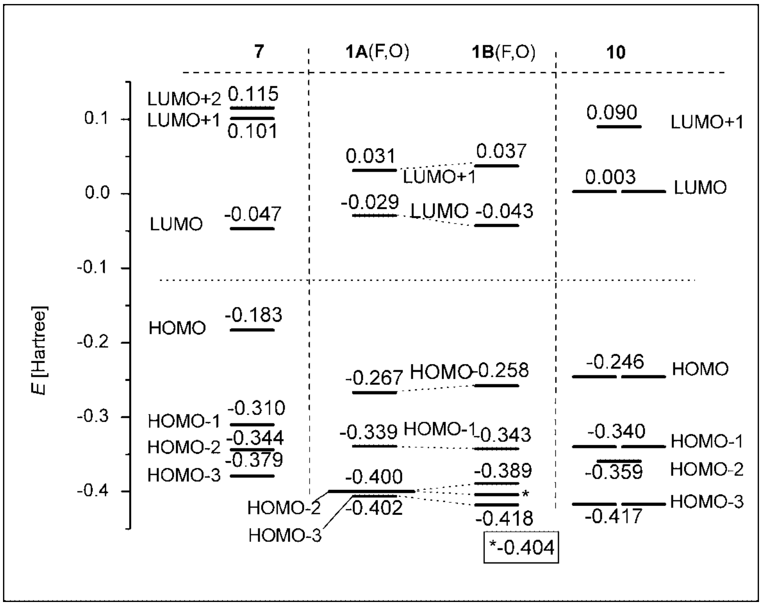

Figure 7. Schematic representation of the MO energy levels for **7**, **10**, **1A**(F,O) and **1B**(F,O) computed at the B3LYP/6-31G(d) level of theory.

ping p_z orbitals that lead to a system that may be regarded as having “homogenic” antiaromaticity. In the case of **1A**, the overlapping orbitals could in principle be composed of three p_z AO of Y^2, C^3 and C^4, and some appropriately oriented d-AO of P^1. Therefore, this type of interaction could perhaps be referred to as “heterogenic” antiaromaticity (Figure 6), analogous to the phenomenon of heterogenic aromaticity. In the case of **1B**, this conjugation between the axial Y^2 and P^1 is perhaps not significant and therefore this compound must be nearly nonaromatic.

The types of computed molecular orbitals (MO) for **1A**(F,O) and **1B**(F,O) are shown in Figure 7 and Figure S1. The MOs of **1A**(F,O) show a significant correlation with the MOs of antiaromatic **7**, for example the shape of the HOMO of **1A**(F,O) is similar to the HOMO of **7** but with different AO coefficients (Table S2). During the pseudorotation of the molecule from structure **1A** to **1B**, the arrangement around the P atom changes. This causes an alteration in the molecular symmetry as well, which leads to different MOs; therefore, the MOs of **1B**(F,O) show significant alteration form the MOs of **1A**(F,O) and **7**, both in their shape and their order of energy levels (Figure 7). The shape of the HOMOs of **1A**(F,O) and **1B**(F,O) markedly differ from each other, which reflects the different electronic structures and related molecular properties. For the sake of comparison, the MO energy levels of aromatic benzene (**10**) are also presented in Figure 7.

Although these destabilizing antiaromatic effects can partially be attributed to the d orbitals, it is unusual in the case of higher row elements.[21] Nevertheless, previous results predicted a significant stabilizing effect when the d shell is introduced.[22,23] In the case of **1**(F,O), the introduction of the d shell also decreases the overall energy level of the compounds examined, but to a different extent for **1A** and **1B**. The differences between the energies of **1A** and **1B** computed at the B3LYP/6-31G and B3LYP/6-31G(d) levels of theory are –584.18 and –588.48 kJmol, respectively, which implies that **1B** is more stable than **1A** by 4.30 kJmol, and that **1B**, in fact, becomes more antiaromatic. The AO coefficients also indicate (Table S2) that there is a relatively large contribution from the p_z orbital. Coefficients that are an order of magnitude smaller also indicate that d-type AOs of, Y^2, C^3 and C^4 are involved as well. However, the contribution from the d-type AO of P^1 to the highest π-type MO (HOMO) is small and about the same for both **1A** and **1B**.

Finally, one may describe the chemical structures of **1A** and **1B** by the resonance structures in Figure 8, which is an extended version of Figure 5. The charged resonance structure for **1B** is very typical.

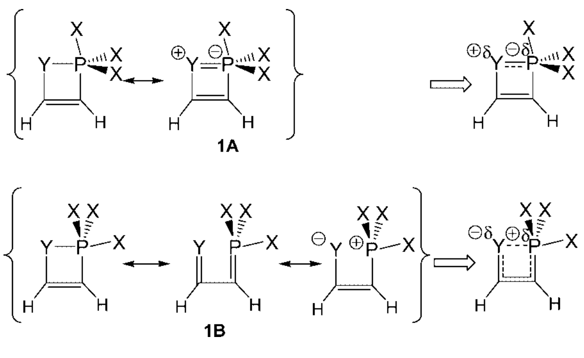

Figure 8. Resonance and the resulting structures for compound **1A** and **1B**.

Enthalpies of Hydrogenation

According to the linear aromaticity and antiaromaticity scale,[6] in all cases, heterophosphetes **1A** produce more exothermic ΔH_{H2} values than **1B**, which alludes to the more

Table 2. Computed ΔH_{H2} and $\Delta\Delta H_{H2}$values in kJ mol^{-1} at the B3LYP/6-311++G(2d,2p) level of theory and the extent of antiaromaticity (–) or aromaticity (+) measured in % for **1**.

		1A				**1B**				
		ΔH_{H2}[A] **1A**(X,Y) → **2A**(X,Y)	ΔH_{H2} **1A**(X,CH$_2$) → **2A**(X,CH$_2$)	$\Delta\Delta H_{H2}$ **1A**	%	ΔH_{H2}[B] **1B**(X,Y) → **2B**(X,Y)	ΔH_{H2} **1B**(X,CH$_2$) → **2B**(X,CH$_2$)	$\Delta\Delta H_{H2}$ **1B**	%	ΔH_{H2}[**B**] – ΔH_{H2}[**A**]
	F	–161.58	–121.53	–40.05	–27.60	–118.69	–111.44	–7.25	–5.54	42.89
O	Cl	–153.95	–119.34	–34.61	–23.95	–107.97	–113.23	5.26	2.87	45.98
	CN	–153.20	–119.19	–34.01	–23.54	–99.81	–110.00	10.19	6.19	53.39
			Average:		–25.03		Average:		1.17	47.42
	F	–171.10	–121.53	–49.57	–34.01	–125.79[a]	–111.44	–14.35	–10.32	45.31
NH	Cl	–164.41	–119.34	–45.07	–30.98	–119.61[a]	–113.23	–6.38	–4.96	44.80
	CN	–159.43	–119.19	–40.24	–27.73	–102.80[a]	–110.00	7.20	4.17	56.63
			Average:		–30.91		Average:		–3.70	48.91
	F	–148.31	–121.53	–26.78	–18.68	–115.95[a]	–111.44	–4.51	–3.70	32.36
S	Cl	–142.25	–119.34	–22.91	–16.08	–107.04[a]	–113.23	6.19	3.50	35.22
	CN	–141.62	–119.19	–22.43	–15.75	–95.27[a]	–110.00	14.73	9.24	46.35
			Average:		–16.84		Average:		3.01	37.97
			Overall average:		–24.26		Overall average:		0.16	44.77

[a] **2B** structure is forced with fixed torsion angle.

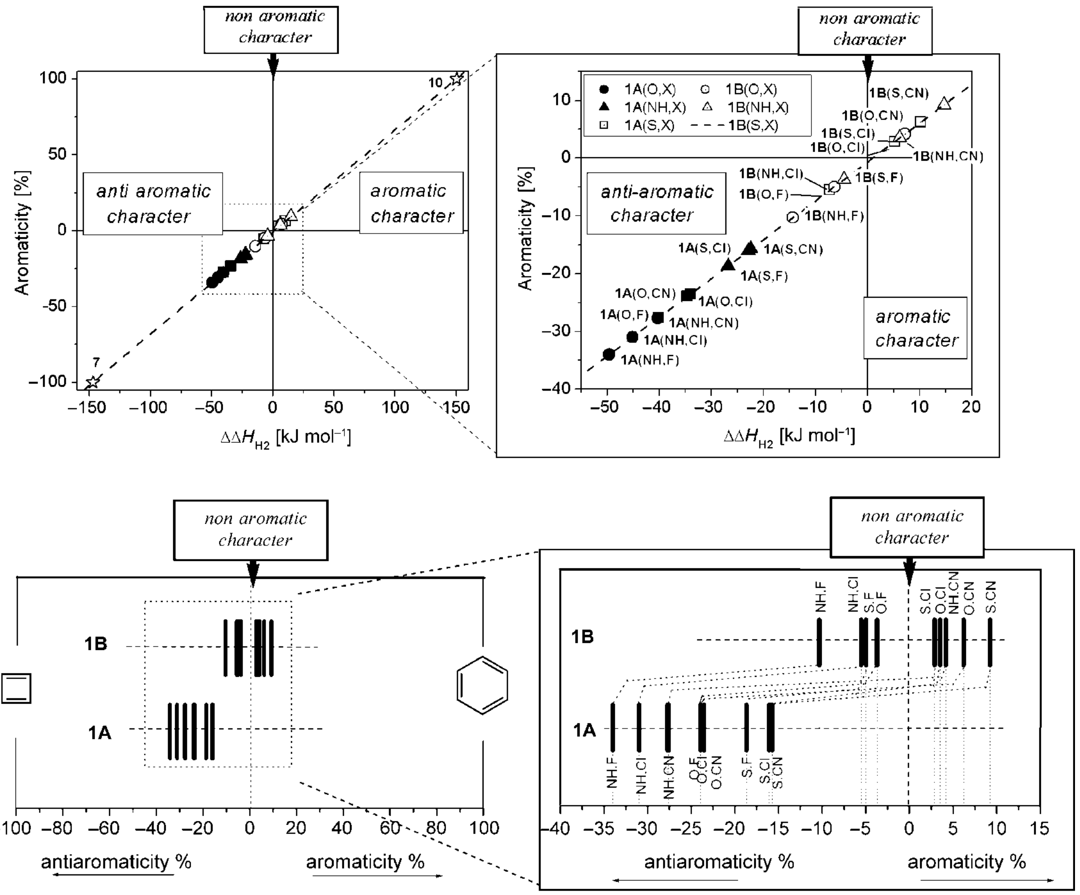

Figure 9. Computed aromaticity and antiaromaticity scale for **1A** and **1B** computed at the B3LYP/6-311++G(2d,2p) level of theory.

significant antiaromatic character of **1A**. Heterophosphetes **1B** exhibit ΔH_{H2} values that are close to the reference values, which suggests that species **1B** belongs to the nonantiaromatic class of compounds (Table 2, Figure 9). By applying this concept, heterophosphetes **1A** can be characterised by a significant degree of (–15.75%) – (–34.01%) antiaromaticity, whereas compounds **1B** have values of only (9.24%) – (–10.32%) and have little aromatic character. One may recognize that the X substituents and the Y heteroatom significantly influence the degree of antiaromaticity of **1**. The strongest antiaromatic percentage for **1** occurred when Y = NH. When Y = S, however, this resulted in the least significant degree of antiaromaticity. Compound **1** with oxygen as the heteroatom can be placed between the nitrogen and sulphur analogues. With regard to the X substituents, the F group caused the strongest antiaromaticity, as expected, followed by Cl and the series is closed by the CN substituent.

Optimised geometry parameters such as planarity, bond length and bond angles may also confirm the antiaromaticity discussed above. In the case of **1A**(X,NH) and **1B**(X,NH), the N atom is not planar. The N atom is able to alter its hybridisation state from sp^2 to sp^3, which decreases the antiaromatic character that would be observed in the planar structure.

The antiaromaticity of **5′**, which is **5**[12] without the isopropyl groups in the phenyl ring, was also evaluated by way of the hydrogenation reaction (Figure 2). This compound shows –7.43% antiaromaticity, and is virtually nonaromatic. This is most likely due to the large $P^1–Y^2$ bond length (2.46 Å), which efficiently decreased the unfavourable overlapping between these two atoms in the key position. For this reason, this compound could be synthesised.

One may also outline the following thermodynamic cycle shown in Scheme 3 by utilizing the data from Tables 1 and 2, where the difference in $\Delta H_{\mathbf{1A}\rightarrow\mathbf{1B}}$ and $\Delta H_{\mathbf{2A}\rightarrow\mathbf{2B}}$ may also be proportional to antiaromaticity. The equation for the thermochemical cycle may be written as shown in Equation (7). The numbers in the last columns of Tables 1 and 2 are identical.

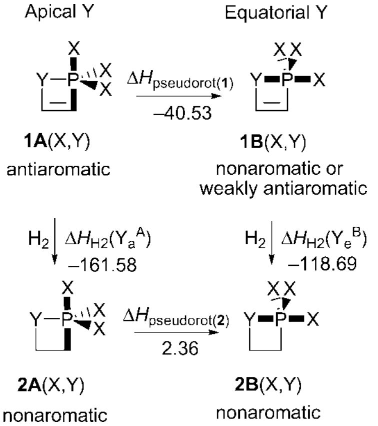

Scheme 3. Born–Haber-type thermochemical cycle. This scheme includes for illustrative purpose various enthalpy values ($kJ\,mol^{-1}$) of compounds with Y = O and X = F.

$$\Delta H_{H2}(Y_a^A) + \Delta H_{pseudorot}(\mathbf{2}) = \Delta H_{pseudorot}(\mathbf{1}) + \Delta H_{H2}(Y_e^B) \qquad (7)$$

It has already been emphasised at the end of the section entitled Electronic Structure that d orbitals do have stabiliz-

Table 3. Computed ΔH_{H2} and $\Delta\Delta H_{H2}$ values in $kJ\,mol^{-1}$ and $P^1–O^2$ atomic distances as well as their differences measured in Å for compounds **1A**(F,O), **1B**(F,O) obtained at various level of theory.[a]

Method	**1A**(F,O)					**1B**(F,O)					
	ΔH_{H2}[A]	ΔH_{H2}[REF]	$d_{P1–O2}$	$\Delta\Delta H_{H2}$	%	ΔH_{H2}[B]	ΔH_{H2}[REF]	$d_{P1–O2}$	$\Delta\Delta H_{H2}$	%	$\Delta d_{\mathbf{1B}–\mathbf{1A}}$
A	–169.54	–149.07	1.874	–23.48	–18.14	–131.33	–135.28	2.026	3.95	–0.25	0.152
B	–164.63	–129.07	1.695	–35.04	–25.64	–124.24	–117.61	1.884	–6.63	–6.83	0.189
C	–161.58	–121.53	1.676	–40.05	–27.60	–121.53	–111.44	1.892	–7.25	–5.54	0.216

[a] A: B3LYP/6-31G; B: B3LYP/6-31G(d); C: B3LYP/6-311++G(2d,2p); ΔH_{H2}[REF] = **1**(F,CH_2) → **2**(F,CH_2).

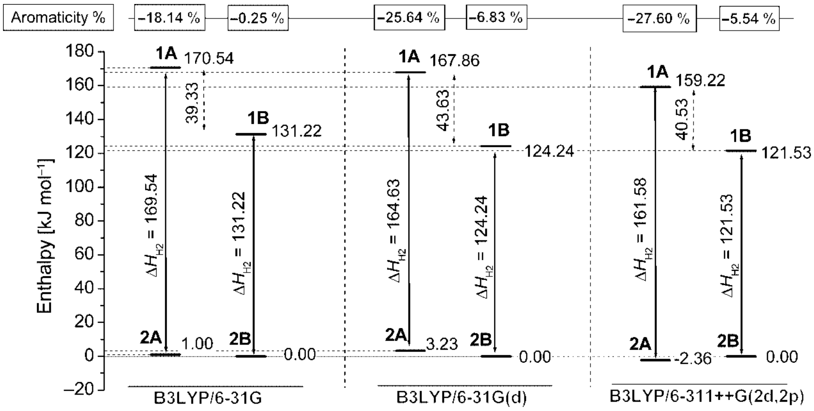

Figure 10. Relative enthalpies of hydrogenation and the resultant % antiaromaticity as a function of the basis set applied.

ing effects. However, the inclusion of one set of d functions do stabilize **1B**(F,O) by 4.30 kJ mol more than **1A**(F,O), so much so that **1A** becomes considerably more antiaromatic than **1B**. For this reason, a basis set study was made by using the 6-31G, 6-31G(d) and 6-311++G(2d,2p) basis sets of atomic functions at the B3LYP level of theory. Enthalpies and relative enthalpies are summarised in Table S3 and Table 3, respectively. The relative stabilities and antiaromatic percentage values are also illustrated in Figure 10.

The geometries are also relevant. As the d orbitals in the molecular computations are included, the P^1–O^2 distance shortens as the antiaromaticity increases (Table 3). The P–F_{apical} bond also shows marked differences for **1A**(F,O) and **1B**(F,O). For the **2A→1A** conversion, the P–F_{apical} bond shrinks only a little (0.006Å), whereas for the **2B→1B** transition, the bond shrinks to more than five times that value (0.033Å). This indicates that **1B** has a more pronounced π-type exocyclic P–F_{apical} interaction than **1A**. Consequently, in **1A** the O–P π-type interaction dominates rather than the π-type exocyclic P–F_{apical} interaction, which is also indicated in Scheme 4.

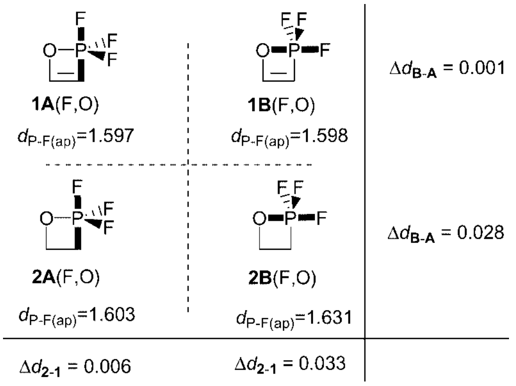

Scheme 4. The P–F_{apical} distance in compounds **1A**(F,O), **1B**(F,O), **2A**(F,O) and **2B**(F,O) and their differences.

Figure 11 is obtained by converting the difference between the PESs of Figure 4 to the energy difference that arises as a result of aromaticity and antiaromaticity on the linear scale[6] as shown in Equations (8), (9) and (10). Note that the value is strongly negative for the geometry of **1A**, which indicates antiaromatic character.

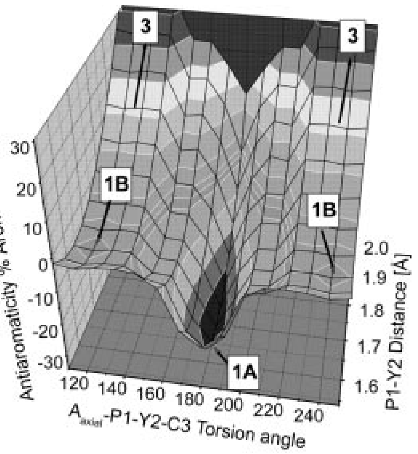

Figure 11. 3D aromaticity (positive) and antiaromaticity (negative) surface of **1**(F,O) as a function of selected internal geometrical parameters (χ,d).

$$\Delta E[\text{examined}(\chi,\text{d})] = E_{\mathbf{2}(X,Y)}(\chi,\text{d}) - E_{\mathbf{1}(X,Y)}(\chi,\text{d}) - E_{H2} \tag{8}$$

$$\Delta E[\text{reference}(\chi,\text{d})] = E_{\mathbf{2}(X,CH_2)}(\chi,\text{d}) - E_{\mathbf{1}(X,CH_2)}(\chi,\text{d}) - E_{H2} \tag{9}$$

$$\text{Aromaticity}(\chi,\text{d}) = m\{\Delta E[\text{examined}(\chi,\text{d})] - \Delta E[\text{reference}(\chi,\text{d})]\} + b \tag{10}$$

The result of Equation (10) is expressed in percentage units (%) and the values for *m* and *b* were defined previously ($m = 0.6496$; $b = -1.9273$).[6]

Thus, in the case of **1**(F,O), conformation **1A** is trapped in an antiaromatic hole, and conformation **1B** is in a valley that is neither really aromatic nor really antiaromatic. In contrast, structure **3** is conjugated so it assumes a low value at the aromatic hill-side.

Conclusions

The present results reveal that heterophosphetes, which exist as two conformers (**1A** and **1B**), are thermodynamically unstable because of their antiaromaticity character that originates form the conjugation of the empty d orbitals of P^1 and the occupied p_z orbital of the Y^2 atom. This type of antiaromaticity is defined as "heterogenic" antiaromaticity. Compounds **1A** with equatorial Y^2 atoms possess larger antiaromatic character (–25%) than compounds **1B** with axial Y^2 atoms (0%); therefore, compounds **1B** can practically be considered as nonaromatic compounds. The thermodynamic stability of **1A** and **1B** has been studied systematically and it was shown that electron-withdrawing groups (F, Cl, CN) on the P^1 atom are able to provide significant stability for both **1A** and **1B**. Each of the overall 3D potential energy surfaces and antiaromaticity % surface of **1**(F,O) has been computed and discussed.

Supporting Information (see footnote on the first page of this article): Schematic representation of selected molecular orbitals of **7**, **1A**(F,O) and **1B**(F,O). Table of P^1–Y^2 atomic distances of **1A**, **1B** and **2**. Structure of **2A**(F, CH_2). Selected AO coefficients of the last two occupied MOs of **1A**(F,O) and **1B**(F,O). Computed enthalpies of **1A**,**B**/**2A**,**B**(X,Y). Computed energies plus zeropoint energies, internal energies and enthalpies for all heterophosphetes. The list of *xyz* geometries of compounds examined at the B3LYP/6-311++G(2d,2p) level of theory

Acknowledgments

The authors wish to thank the Ministry of Education for financial support through the Hungarian Scientific Research Fund (OTKA T67679). T. N. is grateful for a Bolyai Fellowship.

---

[1] G. Maier, *Angew. Chem. Int. Ed. Engl.* **1974**, *13*, 425–490, and references cited therein.

[2] A. Fattahi, L. Lis, Z. Tian, S. R. Kass, *Angew. Chem. Int. Ed.* **2006**, *45*, 4984–4988.

[3] A. Fattahi, L. Lis, S. R. Kass, *J. Am. Chem. Soc.* **2005**, *127*, 3089.

[4] V. I. Minkin, M. N. Glukhotsev, B. Y. Simkin, *Aromaticy and Antiaromaticy: Electronic and Structural Aspects*, Wiley, New York, **1994**.

[5] G. Maier, *Angew. Chem. Int. Ed. Engl.* **1988**, *27*, 309–446, and references cited therein.

[6] Z. Mucsi, B. Viskolcz, I. G. Csizmadia, *J. Phys. Chem. A* **2007**, *111*, 1123–1132.

[7] a) G. Keglevich, H. Forintos, T. Körtvélyesi, *Curr. Org. Chem.* **2004**, *8*, 1245–1261; b) G. Keglevich, T. Körtvélyesi, H. Forintos, S. Lovas, *J. Chem. Soc., Perkin Trans. 2* **2002**, 1645–1646; c) G. Keglevich, H. Forintos, T. Körtvélyesi, L. Tőke, *J. Chem. Soc., Perkin Trans. 1* **2001**, 1–3; d) G. Keglevich, T. Körtvélyesi, H. Forintos, Á.-Gy. Vaskó, I. Vladiszlav, L. Tőke, *Tetrahedron* **2002**, *58*, 3721–3727; e) G. Keglevich, E. Dudás, M. Sipos, D. Lengyel, K. Ludányi, *Synthesis* **2006**, *8*, 1365–1369.

[8] a) T. Uchiyama, T. Fujimoto, A. Kakehi, I. Yamamoto, *J. Chem. Soc., Perkin Trans. 1* **1999**, 1577–1580; b) N. Kano, J. H. Xing, S. Kawa, T. Kawashima, *Tetrahedron Lett.* **2000**, *41*, 5237.

[9] J. A. Altman, K. Yates, I. G. Csizmadia, *J. Am. Chem. Soc.* **1976**, *98*, 1450–1454.

[10] D. J. H. Smith, *Comprehensive Org. Chem. Vol. 2* (Ed.: D. Barton), Pergamon, Oxford, **1979**, ch. 10.4, pp. 1233–1256.

[11] E. Vedejs and C. F. Marth in: *Phosphorus-31 NMR Spectral Properties in Compound Characterization and Structural Analysis* (Eds.: L. D. Quin, J. G. Verkade), VCH, New York, **1994**, ch. 23, p. 297.

[12] N. Kano, A. Kikuchi, T. Kawashima, *Chem. Commun.* **2001**, 2096.

[13] T. Kawashima, T. Iijima, A. Kikuchi, R. Okazaki, *Phoshorus, Sulfur Silicon* **1999**, 144–146; T. Kawashima, T. Iijima, A. Kikuchi, R. Okazaki, *Phoshorus, Sulfur Silicon* **1999**, 149–152.

[14] A. D. Beke, *J. Chem. Phys.* **1993**, *98*, 5648–5651.

[15] M. J. Frisch, G. W. Trucks, H. B. Schlegel, G. E. Scuseria, M. A. Robb, J. R. Cheeseman, V. G. Zakrzewski, J. A. Montgomery, R. E. Stratmann Jr, J. C. Burant, S. Dapprich, J. M. Millam, A. D. Daniels, K. N. Kudin, M. C. Strain, O. Farkas, J. Tomasi, V. Barone, M. Cossi, R. Cammi, B. Mennucci, C. Pomelli, C. Adamo, S. Clifford, J. Ochterski, G. A. Petersson, P. Y. Ayala, Q. Cui, K. Morokuma, D. K. Malick, A. D. Rabuck, K. Raghavachari, J. B. Foresman, J. Cioslowski, J. V. Ortiz, A. G. Baboul, B. B. Stefanov, G. Liu, A. Liashenko, P. Piskorz, I. Komaromi, R. Gomperts, R. L. Martin, D. J. Fox, T. Keith, M. A. Al-Laham, C. Y. Peng, A. Nanayakkara, M. Challacombe, P. M. W. Gill, B. Johnson, W. Chen, M. W. Wong, J. L. Andres, C. Gonzalez, M. Head-Gordon, E. S. Replogle, J. A. Pople, *Gaussian 03*, v.6.0, Gaussian, Inc., Pittsburgh, **2003**..

[16] a) J. Poater, M. Duran, M. Solà, B. Silvi, *Chem. Rev.* **2005**, *105*, 3911–3947; b) T. M. Krygowski, B. T. Stępień, *Chem. Rev.* **2005**, *105*, 3482–3512.

[17] P. v. R. Schleyer, C. Maerker, A. Dransfeld, H. Jiao, N. J. R. von E. Hommes, *J. Am. Chem. Soc.* **1996**, *118*, 6317–6318.

[18] Z. Chen, C. S. Wannere, C. Corminboeuf, R. Puchta, P. v R. Schleyer, *Chem. Rev.* **2005**, *105*, 3842–3888.

[19] a) T. M. Krygowski, K. Ejsmont, B. T. Stępień, M. K. Cyrański, J. Poater, M. J. Solà, *J. Org. Chem.* **2004**, *69*, 6634; b) M. K. Cyrański, P. v. R. Schleyer, T. M. Krygowski, H. J. Jiao, G. Hohlneicher, *Tetrahedron* **2003**, *59*, 1657.

[20] M. Alajarín, P. Sánchez-Andrada, F. P. Cossío, A. Arrietta, B. Lecea, *J. Org. Chem.* **2001**, *66*, 8470–8477.

[21] E. D. Jemmis, K. T. Giju, *Organometallics* **1997**, *16*, 1425–1429.

[22] E. D. Jemmis, B. V. Prasad, *J. Am. Chem. Soc.* **1987**, *109*, 2560–2563.

[23] E. D. Jemmis, R. Hoffmann, *J. Am. Chem. Soc.* **1980**, *102*, 2570–2575.

Received: October 19, 2006